Biosensors and Bioelectronics 41 (2013) 372–378

Contents lists available at SciVerse ScienceDirect

Biosensors and Bioelectronics

journal homepage: www.elsevier.com/locate/bios

Fabrication of GO/PANi/CdSe nanocomposites for sensitive electrochemiluminescence biosensor

Xiao-Wei Hu [a], Chang-Jie Mao [a,*], Ji-Ming Song [a], He-Lin Niu [a], Sheng-Yi Zhang [a], Hai-ping Huang [b,*]

[a] School of Chemistry and Chemical Engineering, Anhui University, Hefei 230039, PR China
[b] Institute of Engineering, Jiangxi University of Science and Technology, Ganzhou 341000, PR China

ARTICLE INFO

Article history:
Received 26 June 2012
Received in revised form
18 August 2012
Accepted 29 August 2012
Available online 5 September 2012

Keywords:
Electrochemiluminescence
GO/PANi/CdSe Nanocomposites
Biosensor

ABSTRACT

A novel graphene oxide sheets/polyaniline/CdSe quantum dots (GO/PANi/CdSe) nanocomposites were successfully synthesized and used for the sensitive electrochemiluminescence (ECL) biosensing. The GO/PANi/CdSe nanocomposites were characterized by transmission electron microscopy (TEM), scanning electron microscopy (SEM), ultraviolet–visible (UV–vis) absorption spectroscopy, photoluminescence (PL) spectroscopy and Fourier transform infrared (FTIR) spectroscopy. Finally, the nanocomposites were employed to construct the biosensor via layer-by-layer assembly for the ECL detection of Cytochrome C (Cyt C). The whole process was characterized by cyclic voltammogram (CV) and electrochemical impedance spectroscopy (EIS). Experimental parameters such as the ratio of GO/PANi, the $K_2S_4O_8$ concentration and the pH value of electrolyte solution were studied to investigate the effect on the ECL intensity. Under the optimized conditions, the ECL intensity decreased linearly with the Cyt C concentrations in the range from 5.0×10^{-8} to 1.0×10^{-4} M with detection limit of 2.0×10^{-8} M. Besides, the as-proposed biosensor exhibits high specificity, good reproducibility, and stability, and may be applied in more bioanalytical systems.

1. Introduction

In the past few years, graphene has attracted more and more attentions and been widely studied since its discovery in 2004 (Novoselov et al., 2004). As a new type of carbon-based nanomaterial with single-atom thickness, graphene exhibits excellent properties such as good thermal and electrical conductivity, high surface area, and strong mechanical strength (Stampfer et al., 2008; Li and Kaner, 2008a). What's more, graphene could promote electron transfer kinetics for a wide range of electroactive species. All these properties make graphene a good candidate in many fields. Graphene oxide (GO) is a chemically modified graphene sheet, which contains a wide range of oxygen functional groups such as epoxide, alcohol, and carboxylic acid both on the basal planes and at the edges of the sheets (Cai et al., 2008). Compared with graphene, GO not only owns the two-dimensional structure, but possesses some unique properties totally different from the graphene. With the existent of these oxygen functional groups, GO could be easily modified to produce homogeneous colloidal suspensions and to synthesize the graphene-based materials (Park et al., 2009b). Nowadays, GO has been widely applied in nanoelectronics (Savchenko, 2009), electrochemical sensors and biosensors (Liu et al., 2012c; Wang et al., 2009d), lithium battery (Wang et al., 2009a), and supercapacitor (Zhang et al., 2012) *etc.* On the other hand, various GO-based nanocomposites have also been synthesized and used to construct the biosensor. Polystyrene (Hu et al., 2010), polyaniline (Sheng et al., 2011), Au nanoparticles (Gutés et al., 2012), platinum nanoparticles (Dong et al., 2010), and Ag_2S (Mo et al., 2012) are used to prepare the GO based composites and to entrap enzymes and proteins for biosensing, which includes glucose oxidase (Shan et al., 2010), hemoglobin (Feng et al., 2012b), myoglobin (Guo et al., 2012), horseradish peroxidase (HRP) (Zhou et al., 2010), DNA (Mohanty and Berry, 2008), and so on.

Quantum dots (QDs), as newly developed inorganic fluorescent materials, have been extensively studied because of their special optical and electrochemical properties (Burda et al., 2005). After Bard's group found that QDs could generate stable light emission under electrochemical inducement, which was called electrochemiluminescence (ECL), highly luminescent QDs gained increasing attention for the applications in bioconjugates and optical biosensor (Choi et al., 2006; Feng et al., 2007a). In order to gain higher efficient ECL intensity, some oxidants including $K_2S_2O_8$ (Jie et al., 2008a), Na_2SO_3 (Liu and Ju, 2008b) were usually employed in previous reports. But these oxidants would destroy the buffer condition and even oxidize all of the analytes, which made the systems lose selectivity and biocompatibility. In order to overcome this drawback, Li's group (Wang et al., 2009e) reported a graphene oxide amplified electrochemiluminescence (ECL) of quantum dots (QDs) platform. In

* Corresponding authors. Tel./fax: +86 551 3861 279.
E-mail addresses: maochangjie@sina.com (C.-J. Mao), njuhhping@gmail.com (H.-p. Huang).

0956-5663/$ - see front matter © 2012 Elsevier B.V. All rights reserved.
http://dx.doi.org/10.1016/j.bios.2012.08.054

this system, the GO could facilitate the generation of QDs radicals and form a high yield of QDs*, which lead to 5 times enhancement of ECL intensity compared with the system without graphene oxide. Lately, Ju's group (Deng et al., 2011) developed a signal amplification system for QDs by using electrochemically reduced graphene oxide (ERGO). In the presence of dissolved O_2 as coreactant, the QDs/ERGO modified electrode showed ECL intensity increase by 4.2 and 178.9 times as compared with intrinsic QDs and QDs/GO modified electrodes due to the adsorption of dissolved O_2 on ERGO and the facilitated electron transfer. When used for choline and acetylcholine detection, the two ECL biosensors showed the linear response ranges and detection limits of 10–210 μM and 8.8 μM for choline, and 10–250 μM and 4.7 μM for acetylcholine, respectively. As a traditional polymer, polyaniline (PANi) has attracted many interests (Pan et al., 2006; Gangopadhyay and De, 2000) because of its relatively easy preparation and high degree of conductivity.

Cyt C, about 12 kDa molecular weight, is a heme protein involved in mitochondrial electron transfer. It has been widely studied due to its applications for biosensor (Luo et al., 2009) and biofuel cells (Ramanavicius and Ramanaviciene, 2009). Many techniques including electrochemistry (Wang et al., 2012b), fluorescence (Fan et al., 2002), and electrochemiluminescence (Wang et al., 2012c) have been employed for the determination of Cyt C. ECL has special advantages over other analytic techniques, such as low cost, wide range of analytes, and high sensitivity (Li et al., 2011c). Herein, we prepare the GO/PANi/CdSe nanocomposites used for the ECL detection of Cyt C. The GO/PANi nanocomposites were obtained via polymerization of aniline monomer with GO by using $(NH_4)_2S_4O_8$ as oxidant. The GO/PANi/CdSe nanocomposites were received by mixing GO/PANi solution and the CdSe QDs solutions under mild sonication. When the as-prepared nanocomposites were employed to construct the biosensor via layer-by-layer assembly for the ECL detection of Cyt C, the biosensor exhibited wide linear range, good reproducibility and stability.

2. Experimental

2.1. Materials and reagents

Graphite powder (99.995%), potassium permanganate ($KMnO_4$), sodium nitrate ($NaNO_3$), and L-Cysteine were purchased from Shanghai Chemical Reagent Co. Ltd. Aniline was obtained from Sinopharm. Chemical Reagent Co. Ltd. Sulfuric acid (H_2SO_4) was purchased from Shanghai Suyi chemical reagent Co. Ltd. $(NH_4)_2S_4O_8$ was obtained from Guangfu Fine Chemical Research Institute. Cytochrome C (Mw=12,588) was provided by Shanghai Sangon Biological Engineering Technology Co., Ltd. All reagents were used without further purification. 0.1 M PBS of various pH value was prepared by mixing the stock solutions of NaH_2PO_4 and Na_2HPO_4, and adjusting the pH with 0.1 M NaOH and H_3PO_4. 0.1 M PBS (pH 7.4) containing 0.1 M $K_2S_2O_8$ and 0.1 M KCl was used as the electrolyte in ECL test. Ultrapure fresh water which was obtained from AK Exceed-E-V lab pure water system was used throughout this work.

2.2. Synthesis of GO/PANi nanocomposites

Graphene oxide (GO) was prepared from graphite powder by a modified Hummers method (Hummers and Offeman, 1958). A brown suspension of GO (0.5 mg/mL) sheets was obtained by mild sonication of the prepared graphite oxide powder (25 mg) in aqueous 50 mL of 1 M H_2SO_4 for 1 h. Then 200 μL of aniline monomer was added into 50 mL of 0.5 mg/mL of GO solution and sonicated for 30 min. After that, 0.2281 g $(NH_4)_2S_4O_8$ was added into the above mixture and sonicated at 20 °C for 2 h. The GO/PANi nanocomposite was obtained while the color of the mixture changed into black green.

2.3. Preparation of the GO/PANi/CdSe nanocomposites

Scheme 1A shows the whole process for the GO/PANi/CdSe QDs nanocomposites preparation. The L-cysteine modified CdSe quantum dots (QDs) were prepared according to the literature (Park et al., 2009c). To prepare GO/PANi/CdSe nanocomposites, 0.5 mg/mL GO/PANi solution was mixed with CdSe QDs solution with the volume ratio of 1:3 by mild sonication for 5 min.

2.4. Fabrication of ECL biosensor

Scheme 1B shows the strategy of the constructing the ECL biosensor. The whole process can be divided into two sections. First of all, the glassy carbon electrode (GCE, d=4 mm) was carefully polished to a mirror by 1.0, 0.3, and 0.05 μm alumina powder respectively. After sonicating in ethanol and ultrapure water in turn, the electrode was allowed to dry at room temperature. Secondly,

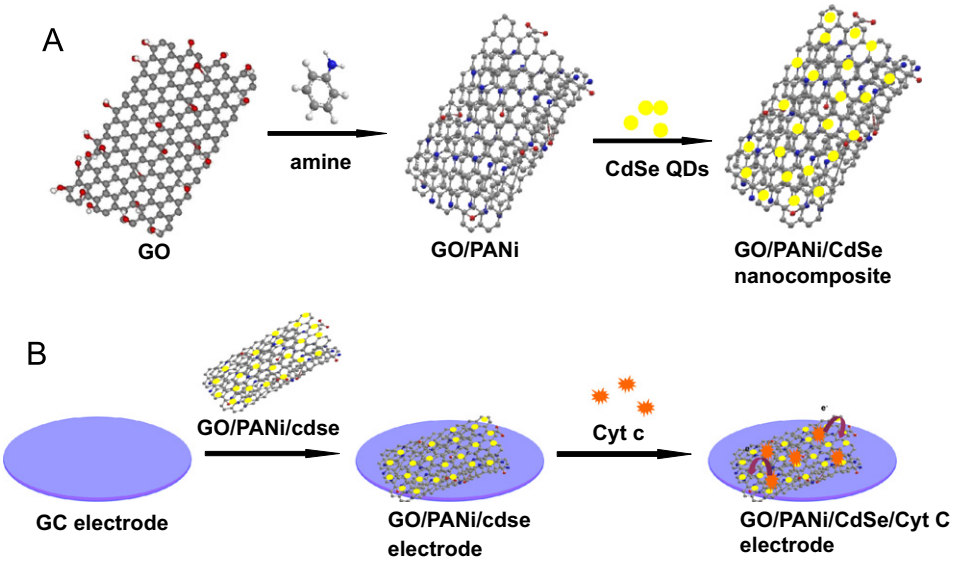

Scheme 1. Schematic representation of preparation procedure of GO/PANi/CdSe nanocomposites (A) and the stepwise biosensor (B).

10 μL of GO/PANi/CdSe nanocomposites solution was dropped onto GCE so as to construct the GO/PANi/CdSe electrode. Then 3 μL of Nafion solution (0.1 wt%) was dropped onto the surface of the GO/PANi/CdSe modified electrodes and dried in air.

2.5. Instruments

The morphology and structural properties were characterized by field emission scanning electron microscopy (SEM, S4800, Hitachi, Japan) and transmission electron microscopy (TEM, JEM-2100, JEOL, Japan). Ultraviolet–visible (UV–vis) absorption spectra were recorded on a UV spectroscopy (UV-3600, Shimadzu, Japan). Photoluminescence (PL) spectra were obtained on photoluminescence spectrometer (F-2500, Hitachi, Japan). Fourier transform infrared (FTIR) spectra were received by a spectrophotometer (870 FTIR, Nicolet Nexus, USA). The electrochemical and electrochemiluminescence (ECL) experiments were conducted by electrochemistry work station (LK2005A, Tianjin, China) and electrochemiluminescence analyzer (MPI-A, Xi'An Remax Electronic Science & Technology Co. Ltd., China) with a conventional three-electrode system composed of a platinum wire as the counter electrode and a saturated calomel electrode (SCE) as the reference; working electrodes were bare or modified glass carbon disk (GCE) electrodes (4 mm diameter), respectively. Electrochemical impedance spectra (EIS) were carried out with a Thales electrochemical workstation (Zahner-elektrik GmbH & Co. KG, Germany), using the same three-electrode system as in the ECL detection.

3. Results and discussion

3.1. Characterization

The morphologies and size of all samples are observed by TEM and SEM techniques. It can be observed in Fig. 1a that the GO nanosheets represent almost a transparent flake-like morphology with thickness of about 10 nm (Fig. 1b). In addition, the restacked parts and wrinkles can also be seen due to the electronic repulsion between the soft and flexible layers. The TEM image in Fig. 1c shows that the edge of GO/PANi nanocomposites is almost transparent, while the center section is very black, corresponding to GO nanosheets and GO/PANi nanocomposites respectively. However, the surface of GO/PANi nanocomposites is very rough and the thickness of single GO/PANi nanocomposites is about 30 nm (Fig. 1d), which is very different from that of GO nanosheets. Moreover, the morphology of the as-prepared GO/PANi nanocomposites is quite uniform and no individual GO or PANi agglomerates can be observed in Figs. 1c and d, indicating that PANi has coupled onto the GO nanosheets completely and successfully. As shown in Fig. 1e, the homogeneous CdSe QDs on the surface of the GO/PANi nanocomposites were

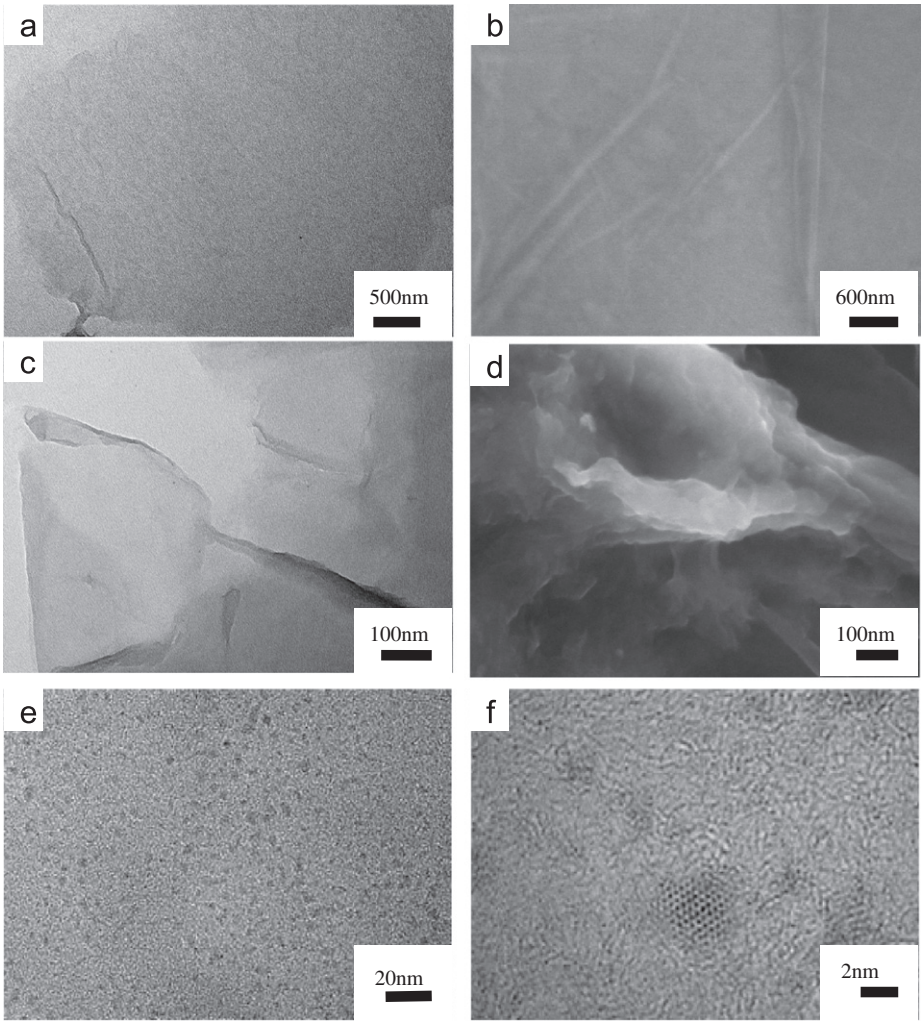

Fig. 1. TEM and SEM images of GO (a and b); GO/PANi nanocomposites (c and d); TEM of GO/PANi/CdSe nanocomposite (e and f).

observed. High-resolution transmission electron microscopy (HRTEM) image (Fig. 1f) displays the crystalline features of CdSe QDs with average size of about 2.5 nm.

Fig. 2A shows the photographs of nanocomposites solution of GO/PANi and GO/PANi/CdSe. It is obviously that the color of GO/PANi (b) is black green. After CdSe QDs added, the color becomes yellow green (d). The result further confirmed that GO/PANi/CdSe nanocomposites was obtained successfully.

FTIR, UV–vis and PL techniques were used to characterize the as-obtained GO/PANi/CdSe nanocomposites. FTIR spectra as shown in Fig. 2B provide further information for GO/PANi/CdSe nanocomposites. As for curve a in Fig. 2B, the spectrum of GO illustrates the presence of C–O (1110 cm^{-1}), C–OH (1395 cm^{-1}), C=O (1733 cm^{-1}), and C–O–C (960 cm^{-1}). The peak at 1631 cm^{-1} can be attributed to the stretching deformation vibration of intercalated water and the skeletal vibrations of unoxidized graphite. The spectrum also shows a broad, intense band at 3410 cm^{-1} that corresponds to O–H stretching vibrations of the O–H groups originated from carboxylic acid as well as intercalated water. This is in agreement with the reported data (Park et al., 2009a; Li et al., 2008b). However, compared with the above bands of GO nanosheets, these absorption bands are decreased in that of the GO/PANi nanocomposites, indicating most of the functional groups have been essentially removed in polymerization process. As shown in curve b of Fig. 2B, the main peaks at 1562 and 1468 cm^{-1} can be assigned to the stretching vibrations of quinono and benzene rings, respectively. The peaks at 1292 and 1227 cm^{-1} correspond to the C–N stretching vibration. The in-plane bending of C–H is reflected in the 1111 cm^{-1} peak. The peak at 790 cm^{-1} is attributed to the out-of-plane bending of C–H. All of the above peaks can be seen from spectrum of GO/PANi nanocomposite film, which indicated that PANi was existent in the surface of GO nanosheets. Furthermore, the absorption bands between 1000 cm^{-1} and 1500 cm^{-1} are almost vanished in the FTIR spectrum of the GO/PANi/CdSe nanocomposites (curve c in Fig. 2B). This indicated the existence of CdSe QDs in the surface of GO/PANi.

In the UV–vis spectra, there are two absorption features of GO in curve a of Fig. 2C. A peak at 230 nm originated from the $\pi \rightarrow \pi^*$ transition of C=C, and a shoulder at about 290 nm corresponded to the $n \rightarrow \pi^*$ transition of the C=O bond. The peak position of polyaniline appeared at 360 and 800 nm in curve b of Fig. 2C, which can be attributed to polaron–π^* and π–polaron transitions respectively. The peak position of GO/PANi nanocomposites spectrum (curve c in Fig. 2C) was the same as polyaniline, but with different absorbance intensity. This transfer indicated that the function groups of GO and PANi had been changed through the in situ reaction. Curve d in Fig. 2C shows that the exact absorption of free CdSe QDs with the same quantity of QDs in the GO/PANi/CdSe nanocomposites. The absorption position located at 420 nm, which means the size of CdSe QDs was 1.72 nm. And the weak peak at about 360 nm is attributed to the absorption of the particles with smaller size. Compared with CdSe QDs, the absorption peak at 420 nm (curve e in Fig. 2C) of GO/PANi/CdSe nanocomposites is much weaker than that of CdSe QDs, which indicates that the CdSe QDs have been combined with GO/PANi nanocomposites.

The PL emission spectra of the products are shown in Fig. 2D. There were very weak emission peak in the GO nanosheets, PANi and GO/PANi nanocomposites. The peak position of pure CdSe QDs was 522 nm (curve d in Fig. 2D). The peak position of GO/PANi/CdSe QDs was 523 nm (curve e in Fig. 2D), which was almost identical to pure CdSe QDs, except for little decrease in emission intensity. This result can be attributed to the electron transfer from excited CdSe QDs to GO/PANi nanocomposite. The 1 nm red shift suggested that the light emission feature of CdSe

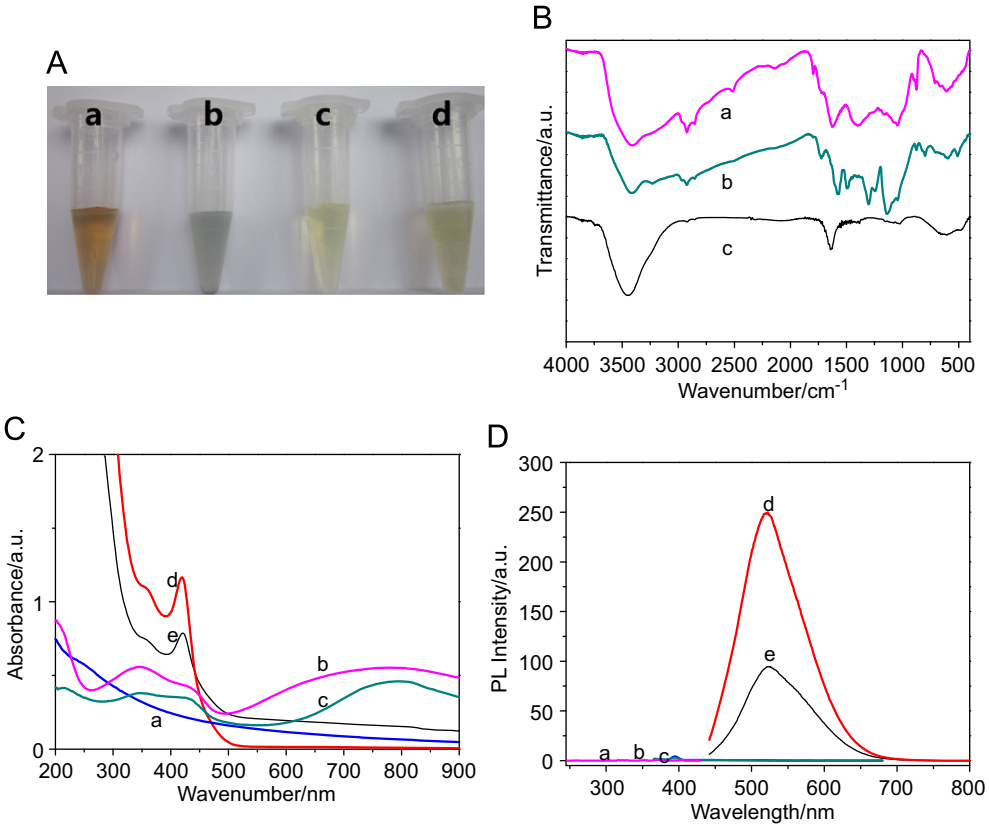

Fig. 2. (A) Images of water dispersions of (a) GO, (b) GO/PANi, (c) CdSe and (d) GO/PANi/CdSe; (B) FTIR spectra of (a) GO; (b) GO/PANi; (c) GO/PANi/CdSe. (C) UV–vis spectra of (a) GO; (b) PANi; (c) GO/PANi; (d) CdSe; (e) GO/PANi/CdSe; (D) PL spectra of (a) GO; (b) PANi; (c) GO/PANi; (d) CdSe; (e) GO/PANi/CdSe.

QDs was preserved by depositing them on the surface of the GO/PANi nanocomposites. PL spectra reveal that GO/PANi/CdSe nanocomposite have been obtained.

3.2. The electrochemical and ECL behavior

EIS is an effective method to monitor the feature of modified electrode surface. It consists of two portions: the semicircle portion and the linear portion. The semicircle diameter at higher part represents the electron-transfer resistance (R_{et}), and the linear part at lower frequencies represents the diffusion process. Fig. 3A shows the Nyquist plots of EIS observed upon the stepwise modification processes. The bare glass electrode revealed a small semicircle domain, which implies the lowest electron-transfer resistance (curve a in Fig. 3A). Comparing with curve a in Fig. 3A, semicircle diameter in curve b of Fig. 3A is slightly increased due to the introduction of GO/PANi nanocomposites. Additionally, EIS of the GO/PANi/CdSe nanocomposites modified electrode shows a large increase in diameter (curve c in Fig. 3A), suggesting that the CdSe QDs formed an additional barrier and further prevented the transformation of electron to the electrode surface.

Fig. 3B shows the ECL-potential curves obtained by the electrodes modified with different products, respectively. Obviously, the bare GCE and the GO/PANi nanocomposites modified electrode have poor ECL emission (curves a and b in Fig. 3B). However, all electrodes containing CdSe QDs have good ECL emission peak (curves c and d in Fig. 3B). Compared with curve c in Fig. 3B, the intensity of curve d in Fig. 3B has been enhanced obviously. The ECL intensity of the GO/PANi/CdSe nanocomposites is over four times higher than the intensity of pure CdSe QDs. The result reveals that the introduction of GO/PANi nanocomposite enhanced the ECL emission. This may be due to the fact that the larger surface area in the nanocomposite film not only induced the occurrence of ECL signal at the interface, but also in the nanocrystalline film. Furthermore, the amine groups of GO/PANi nanocomposite facilitated the radical generation and electron-transfer processes during the ECL reaction. In addition, the strong ECL emission produced by the GO/PANi/CdSe nanocomposites is very stable under successive cyclic voltammetry (inset in Fig. 3B). All the ECL peaks in the absence of CdSe QDs were very low, which indicated that ECL was from the CdSe QDs. Thus, This ECL mechanism is similar to that of the other nanomaterials (Ding et al., 2002). In our case, when the potential became sufficiently negative, the CdSe QDs was reduced by electron injetion to nanocrystalline species ($CdSe^{-\bullet}$). Meanwhile, the reduction of $S_2O_8^{2-}$ by GO/PANi (R-NH_2) on the electrode produces a strong oxidant ($SO_4^{-\bullet}$). Then $CdSe^{-\bullet}$ could react with $SO_4^{-\bullet}$ to emit light in the aqueous solution. The ECL mechanism is listed as follows (Zu and Bard, 2000; Jie et al., 2008b):

$$CdSe\ QDs + ne^- \rightarrow nCdSe^{-\bullet} \quad (1)$$

$$S_2O_8^{2-} + R-NH_2 \rightarrow SO_4^{2-} + SO_4^{-\bullet} + R-NH_2^{+\bullet} \quad (2)$$

$$CdSe^{-\bullet} + SO_4^{-\bullet} \rightarrow CdSe^* + SO_4^{2-} \quad (3)$$

$$CdSe^* \rightarrow CdSe + h\nu \quad (4)$$

3.3. Condition optimization

The effects on ECL responses were studied by a series of experiments parameters. Fig. 4A shows the effect of the volume ratio of GO/PANi to CdSe on ECL intensity. When the $V_{CdSe}/V_{GO/PANi}$ was increased to 3, the nanocomposites gained the maximum ECL intensity. This explain that increasing CdSe QDs would efficiently facilitate the radical generation, and lead to the enhancement in ECL intensity. However, the ECL intensity decreased dramatically with $V_{CdSe}/V_{GO/PANi}$ over 3, which indicated that deposition of a large amount of CdSe QDs on the electrode surface (Jie et al., 2008b). Thus $V_{CdSe}/V_{GO/PANi}$ for biosensors was chosen to be 3.

The effect of pH value on the ECL response was investigated in the range of 4.0–9.0. As shown in Fig.4B, the ECL response of the biosensor increased from 4.0 to 7.0 and then decreased. The maximum ECL intensity was observed at pH 7.0. The influence of pH value on the ECL response may be explained as follows. With the increasing pH value in the range from 4.0 to 7.0, the more negatively charged species could accelerate electron transfer. However, when pH was higher than 7.0, excessive anions would be loaded on the surface of the electrode, which extremely suppressed the approach of negatively charged of CdSe QDs and made the ECL intensity decrease quickly (Liu et al., 2007a). Since the optimal pH value for the biological systems is about 7.4, the ECL detection is performed in pH 7.4 PBS containing 0.1 M KCl and 0.1 M $K_2S_2O_8$.

In addition, the effect of $K_2S_2O_8$ concentration on the ECL intensity was also studied in the range from 0.02 M to 0.16 M (Fig. 4C). With the increasing concentrations of $K_2S_2O_8$, the ECL intensity increased. This may be explained that the formed oxidant increased with the increase of $K_2S_2O_8$ density, and

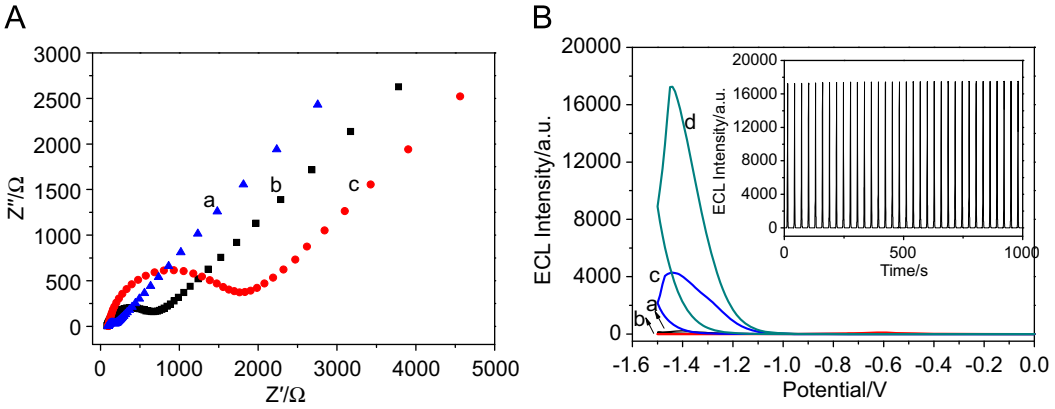

Fig. 3. (A) The ECL-potential curves of different electrodes: (a) bare GCE; (b) GO/PANi/GCE; (c) CdSe/GCE; (d) GO/PANi/CdSe/GCE. (B) Electrochemical impedance spectroscopy of the electrode at different stages: (a) bare GCE; (b) after immobilization of GO/PANi nanocomposites; (c) after assembly of GO/PANi/CdSe nanocomposites in 0.1 M KCl solution with 4 mM $[Fe(CN)_6]^{3-/4-}$ electroactive probes. The frequency range in EIS experiments is between 10^2 Hz and 10^5 Hz with signal amplitude of 5 mV.

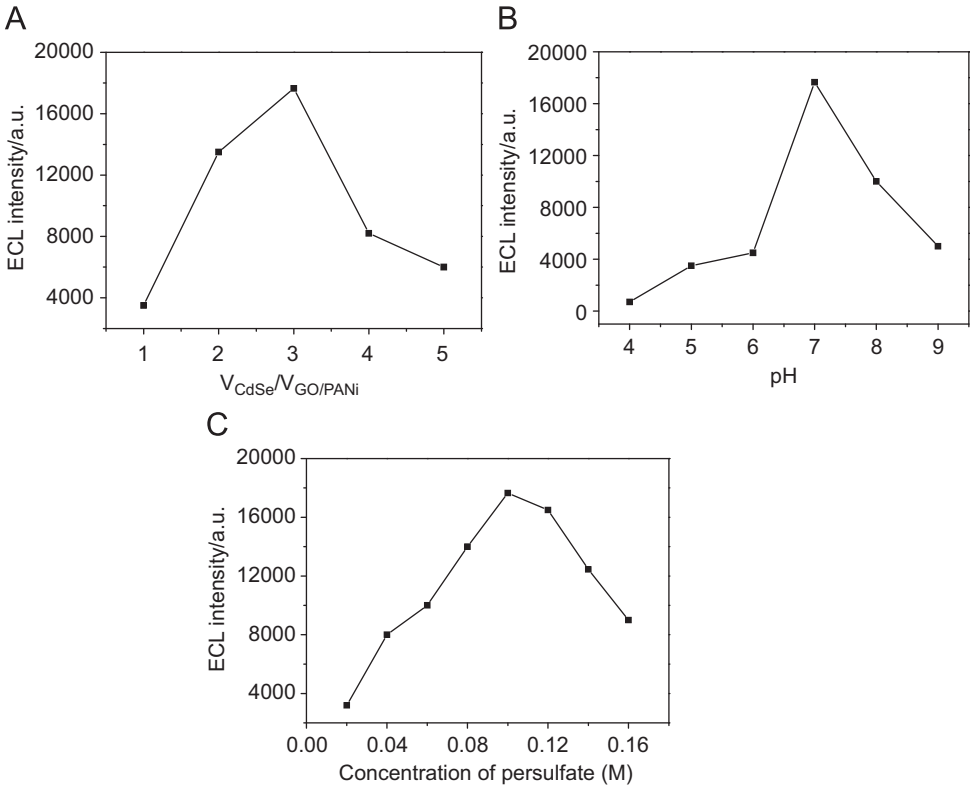

Fig. 4. The effects of experiment parameters on the GO/PANi/CdSe nanocomposites ECL response: (A) the volume ratio of GO/PANi to CdSe (V:V); (B) the pH value; and (C) the $K_2S_2O_8$ concentration.

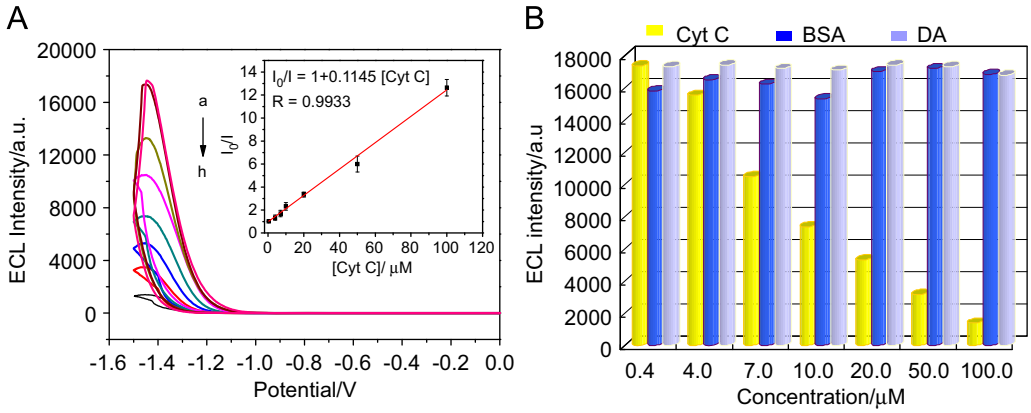

Fig. 5. (A) ECL intensity changes with Cyt C concentrations (μM): (a) 0.0; (b) 0.4; (c) 4.0; (d) 7.0; (e)10.0; (f) 20.0; (g) 20.0; (h) 100.0; inset: calibration curve for Cyt C determination; (B) contract test results with ECL sensor.

leading to enhancement in ECL intensity. When $K_2S_2O_8$ exceeded 0.1 M, the ECL intensity decreased, which indicated that the overloaded $SO_4^{-\bullet}$ increased the film thickness. Thus, the 0.1 M $K_2S_2O_8$ is selected for the ECL detection.

3.4. ECL detection of Cyt C

When Cyt C was injected into electrolyte, the ECL intensity dramatically decreased. The more Cyt C concentrations that was increased, the more ECL intensity that was decreased. The reason was that Cyt C increased the steric hindrance which inhibited the transfer of electrons and $K_2S_2O_8$ in the ECL reaction, and thus decreased the ECL intensity (Jie et al., 2008b). The results suggested that the Cyt C concentration could be determined with the ECL biosensor. Fig. 5A shows the ECL responses upon the increase of different Cyt C concentrations. The ECL intensity decreased linearly with the Cyt C concentrations ranging from 5.0×10^{-8} to 1.0×10^{-4} M (R=0.9933, n=7). The detection limit was estimated to be 2.0×10^{-8} M. In particular, compared with other analytical method, the fabricated ECL biosensor displayed a wider linear detection range and lower detection limit which was lower than the previously reported (Wang et al., 2012b, 2012c).

Selectivity is an important criterion for biosensors. To further study the specificity of the ECL biosensor, the contrast measurement was performed by adding dopamine and bovine serum albumin (BSA) to the ECL electrolyte instead of Cyt C, respectively. Comparing with the quenching effect of Cyt C on ECL intensity, as shown in Fig. 5B, the effect of two contrasts is neglectable when

the concentrations are varied from 5.0×10^{-8} to 1.0×10^{-4} M. Thus, the biosensor had a good selectivity to Cyt C, which makes this biosensor feasible for the determination of real sample.

The reproducibility of the biosensor for Cyt C was evaluated from the response to 4 mM Cyt C at five different electrodes. A series measurements from the batch experiments resulted in a relative standard deviation (RSD) of 5.9%, indicating good electrode-to-electrode reproducibility of the sensor. When the biosensor was stored in pH 7.4 PBS at 4 °C for one week, no apparent change in the same Cyt C concentration was found. The above result indicates that the biosensor has good stability.

4. Conclusions

In this work, a novel GO/PANi composite was successfully synthesized in one step by facile in-situ polymerization using GO and aniline monomer as the raw materials. CdSe QDs were successfully attached to GO/PANi to prepare the GO/PANi/CdSe nanocomposite. The nanocomposites maintain the GO's properties of large specific surface, good conductibility and high stability. In addition, the PANi with excellent biocompatibility has amine groups which can decrease the excitation energy of the ECL reaction of CdSe QDs. The obtained GO/PANi/CdSe nanocomposite was used to construct an ECL biosensor via layer-by-layer assembly. The as-prepared ECL biosensor exhibited high ECL intensity, long-term stability, high sensitivity and excellent specificity to Cyt C. Furthermore, GO/PANi/CdSe nanocomposites could be a promising option for the development of various ECL biosensors.

Acknowledgments

This work was supported by the National Natural Science Foundation of China (Grant nos. 20905001, 21005034 and 21071002), Natural Science Foundation of Anhui Province (11040606Q02) and 211 project and Anhui Province Key Laboratory of Environment-friendly Polymer Materials of Anhui University.

References

Burda, C., Chen, X.B., Narayanan, R., El-Sayed, M.A., 2005. Chemical Reviews 105, 1025–1102.
Cai, W., Piner, R.D., Stadermann, F.J., Park, S., Shaibat, M.A., Ishii, Y., Yang, D., Velamakanni, A., An, S.J., Stoller, M., An, J., Chen, D., Ruoff, R.S., 2008. Science 321, 1815–1817.
Choi, J.H., Chen, K.H., Strano, M.S., 2006. Journal of the American Chemical Society 128, 15584–15585.
Deng, S.Y., Lei, J.P., Cheng, L.X., Zhang, Y.-Y., Ju, H.X., 2011. Biosensors and Bioelectronics 26, 4552–4558.
Ding, Z., Quinn, B.M., Haram, S.K., Pell, L.E., Korgel, B.A., Bard, A.J., 2002. Science 296, 1293–1297.
Dong, L.F., Gari, R.R.S., Li, Z., Craig, M.M., Hou, S.F., 2010. Carbon 48, 781–787.
Fan, C.H., Plaxco, K.W., Heeger, A.J., 2002. Journal of the American Chemical Society 20, 5642–5643.
Feng, C.L., Zhong, X.H., Steinhart, M., Caminade, A.M., Majoral, J.P., Knoll, W., 2007a. Advanced Materials 19, 1933–1936.
Feng, Q.L., Liu, K.-P., Fu, J.-J., Zhang, Y.Z., Zheng, Z.-X., Wang, C.M., Du, Y.L., Ye, W.C., 2012b. Electrochimica Acta 60, 304–308.
Gangopadhyay, R., De, A., 2000. Chemistry of Materials 12, 608–622.
Guo, C.C., Sun, H., Zhao, X.S., 2012. Sensors and Actuators B 164, 82–89.
Gutés, A., Carraro, C., Maboudian, R., 2012. Biosensors and Bioelectronics 33, 56–59.
Hu, H.T., Wang, X.B., Wang, J.C., Wan, L., Liu, F.M., Zheng, H., Chen, R., Xu, C.H., 2010. Chemical Physics Letters 484, 247–253.
Hummers, W.S., Offeman, R.E., 1958. Journal of the American Chemical Society 80 1339–1339.
Jie, G.F., Huang, H.P., Sun, X.L., Zhu, J.J., 2008a. Biosensors and Bioelectronics 23, 1896–1899.
Jie, G.F., Zhang., J.J., Wang, D.C., Cheng, H., Chen, H.Y., Zhu, J.J., 2008b. Analytical Chemistry 80, 4033–4039.
Li, D., Kaner, R.B., 2008a. Science 320, 1170–1771.
Li, D., Muller, M.B., Gilje, S., Kaner, R.B., Wallace, G.G., 2008b. Nature Nanotechnology 3, 101–105.
Li, L.L., Liu, H.Y., Shen, Y.Y., Zhang, J.J., Zhu, J.J., 2011c. Analytical Chemistry 83, 661–665.
Liu, X., Jiang, H., Lei, J.P., Ju, H.X., 2007a. Analytical Chemistry 79, 8055–8060.
Liu, X., Ju, H.X., 2008b. Analytical Chemistry 80, 5377–5582.
Liu, Y.X., Dong, X.C., Chen, P., 2012c. Chemical Society Reviews 41, 2283–2307.
Luo, Y., Liu, H., Rui, Q., Tian, Y., 2009. Analytical Chemistry 81, 3035–3041.
Mo, Z.L., Liu, P.W., Guo, R.B., Deng, Z.P., Zhao, Y.X., Sun, Y., 2012. Materials Letters 68, 416–418.
Mohanty, N., Berry, V., 2008. Nano Letters 8, 4469–4476.
Novoselov, K.S., Geim, A.K., Morozov, S.V., Jiang, D., Zhang, Y., Dubonos, S.V., Grigorieva, I.V., Firsov, A.A., 2004. Science 306, 666–669.
Pan, L.J., Pu, L., Shi, Y., Sun, T., Zhang, R., Zheng, Y.D., 2006. Advanced Functional Materials 16, 1279–1288.
Park, S.J., An, J., Jung, I., Piner, R.D., An, S.J., Li, X., Velamakanni, A., Ruoff, R.S., 2009a. Nano Letters 9, 1593–1597.
Park, S.J., Dikin, D.A., Nguyen, S.T., Ruoff, R.S., 2009b. Journal of Physical Chemistry C 113, 15801–15804.
Park, Y.S., Okamoto, Y., Kaji, N., Tokeshi, M., Baba, Y., 2009c. ACS Nano 4, 121128.
Ramanavicius, A., Ramanaviciene, A., 2009. Fuel Cells 1, 25–36.
Savchenko, A., 2009. Science 323, 589–590.
Shan, C.S., Yang, H.F., Han, D.X., Zhang, Q.X., Ivaska, A., Niu, L., 2010. Biosensors and Bioelectronics 25, 1070–1074.
Sheng, K.X., Bai, H., Sun, Y.Q., Li, C., Shi, G.Q., 2011. Polymer 52, 5567–5572.
Stampfer, C., Schurtenberger, E., Molitor, F., Guttinger, J., Ihn, T., Ensslin, K., 2008. Nano Letters 8, 2378–2383.
Wang, C.Y., Li, D., Too, C.O., Wallace, G.G., 2009a. Chemcial Materials 21, 2604–2606.
Wang, G.X., Qian, Y., Cao, X.X., Xia, X.X., 2012b. Electrochemistry Communications 20, 1–3.
Wang, T., Zhang, S.Y., Mao, C.J., Song, J.M., Niu, H.L., Jin, B.K., Tian, Y.P., 2012c. Biosensors and Bioelectronics 31, 369–375.
Wang, Y., Li, Y.M., Tang, L.H., Lu, J., Li, J.H., 2009d. Electrochemistry Communications 1, 889–1892.
Wang, Y., Lu, J., Tang, L.H., Chang, H.X., Li, J.H., 2009e. Analytical Chemistry 81, 9710–9715.
Zhang, S.L., Li, Y.M., Pan, N., 2012. Journal of Power Sources 206, 476–482.
Zhou, K.F., Zhu, Y.H., Yang, X.L., Luo, J., Li, C.Z., Luan, S.R., 2010. Electrochimica Acta 55, 3055–3060.
Zu, Y., Bard, A.J., 2000. Analytical Chemistry 72, 3223–3232.